

Study of solar sail deformation in zero spin state

Junji Kikuchi, Yoji Shirasawa, Osamu mori, Junichiro Kawaguchi(JAXA)

Abstract

In the period of the reverse spin experiment performed to the solar sail IKAROS, the pictures taken by the monitor cameras imply that the sail became a saddle shape when the spin stopped. It is considered that there are two reasons for it, one is the influence of the plume from the thruster used for the spin-down and the other is the effect of the stiffness of the sail. In this study, by comparing the detailed image analysis of the sail and the simulation using the multi-particle model, the factor of the sail shape change to the saddle shape is investigated.

スピン停止状態におけるソーラーセイルの膜面形状に関する研究

菊池隼仁、白澤洋次、森治、川口淳一郎(JAXA)

摘要

ソーラー電力セイル IKAROS において行われた逆スピン運用の際、モニタカメラから撮像された画像により、スピン停止状態の膜面形状は先端マスを頂点とした鞍形となっていると推測されている。この原因として、スピンドアウン時のスラスト噴射に伴うプルームの影響と、膜面の曲げ剛性の影響の二つが考えられる。本研究では、画像解析によって得られた詳細な膜面形状と、多粒子モデルを用いたシミュレーションの結果を比較することにより、膜面形状が鞍形に変化する要因についての考察を行う。

1. Introduction

Solar sail experimental spacecraft "IKAROS" was launched on May 21, 2010. It is cruising between the Venus and Earth orbit now. Feature of the solar sail is that it is able to deploy the polyimide film of 7.5 μ m by spinning in space. Because the polyimide film reflects the solar pressure, the solar sail can control of attitude and get the thrust. IKAROS is connected to four trapezoidal membranes of about 14m one side. In order to deploy the film surface by using the centrifugal force of the spin, there are tip masses of 0.5kg in each tip interval of petals. After deployment, the solar sail keeps the stretched state by continuing to spin at 1rpm as nominal spin rate,

In order to analyze in detail the behavior of the sail, JAXA conducted two spin operations. First, in a reverse operation, control by thrusters gradually lowers the spin rate, it continues until becoming the opposite spin. Second, in a low spin operation, windmill effect of utilizing the phenomenon that a only solar radiation pressure (SRP) torque lower spin rate naturally is used without spin rate control. Initially, because the centrifugal force is not working in zero spin and there is only the SRP, the solar sail was expected to cause a large deformation in the direction opposite the sun. However, it can be confirmed that the solar sail deformed in a saddle shape from the picture taken by the monitor cameras.

In this study, the factor that the solar sail deformed the saddle shape in zero spin is investigated by using two methods. First, by performing image analysis on pictures taken by monitor cameras, the actual shape of the sail is accurately estimated. Second, by performing a simulation of a multi-particle method which replaces the sail with the spring mass model, the behavior of the sail is estimated analytically. By comparing these two methods, the factor of changing to the saddle shape is investigated.

2. Image Analysis

2-1. Observation equipment

Four monitor cameras are equipped in every 90° of the body as shown in Figure 1. These are called CAM-H1~4. These cameras take the picture from the direction overlooking the sail from the horizontal at 15° depression angle and tip masses which comes in the middle of the screen.

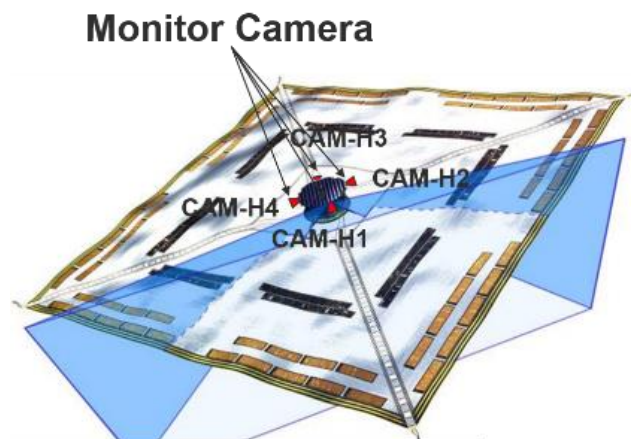


Fig.1 Position of monitor cameras

2-2. Method of Analysis

Image analysis is needed the following two operations; a conversion to two-dimensional pixel coordinates of the image from the three-dimensional coordinates of the inertial system, and correction of a distortion of the monitor camera lens.

First, in this analysis, tip mass which is located in the center of the picture is set as a feature point. Second, the coordinate system of the inertial system is converted to the camera projection plane coordinate system by a coordinate transformation matrix as shown in Figure 2. Third, in consideration of the distortion of the lens, the displacement of the distortion is set from the projection coordinates. Finally, through taking the difference of the coordinate data issued from the calculation and the coordinate data of the position information which has already been obtained, parameters which minimize the error by using the least squares method is defined.

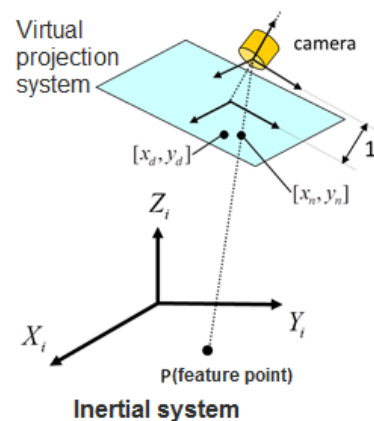


Fig.2 Definition of coordinates

By using this method, it also can be estimated the three-dimensional inertial system coordinates from pixel coordinates data of the picture in reverse. The right of Figure 3 is the result of the calibration test. It can be confirmed that because of the distortion of the lens, a feature point is displaced from the center.



Fig.3 Captured images of the calibration board (left), corrected result (right)

2-3. Image analysis results

Figure 4 is the calibration processed picture taken by CAM-H1 in 1.59rpm. Figure 5 is shown a quantitatively analysis of the z-direction displacement of the tip mass of each petal from the pictures taken from CAM-H1 ~ 4.

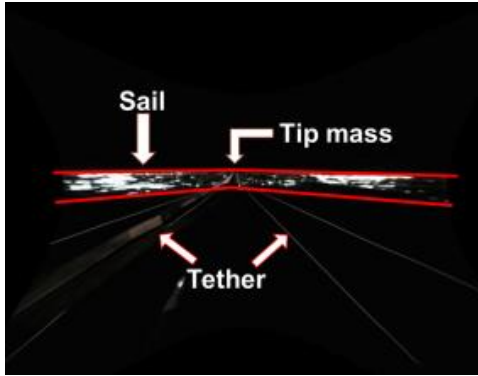


Fig.4 Picture of CAM-H1 in 1.59rpm

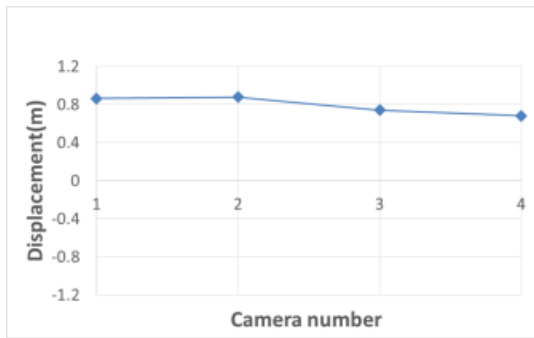


Fig.5 Displacement of tip mass in 1.59rpm

From Figure 5, it can be confirmed that the sail becomes substantially planar. Subsequently, Figure 6 and 7 are shown the picture and the analysis result in 0.055rpm in the low spin operation.

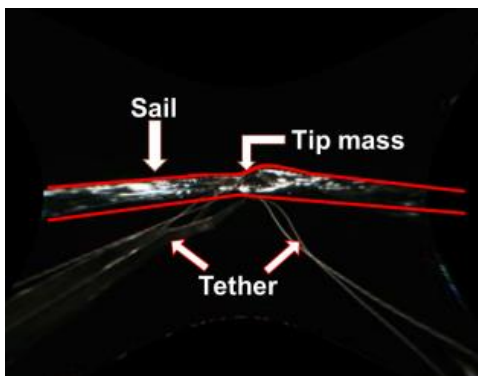


Fig.6 Picture of CAM-H1 in 0.055rpm

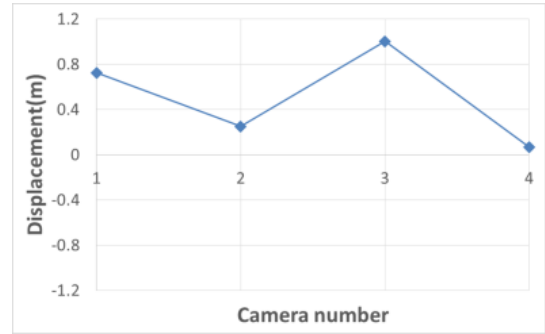


Fig.7 Displacement of tip mass in 0.055rpm

From Figure 6, it can be evaluated that the sail of the picture in 0.055rpm is largely deformed as compared to the picture in 1.59rpm. From Figure 7, the tip masses of the side of CAM-H1 and 3 are displaced upward. On the other hand, the tip masses of the side of CAM-H2 and 4 are displaced downward. In consequent, it can be confirmed that the sail in 0.055rpm changes to the saddle shape.

3. Multi-particle method

In multi-particle model as shown in Figure 8, each element of the membrane is assumed to be isotropic and substituted by particles connected by springs and dampers.

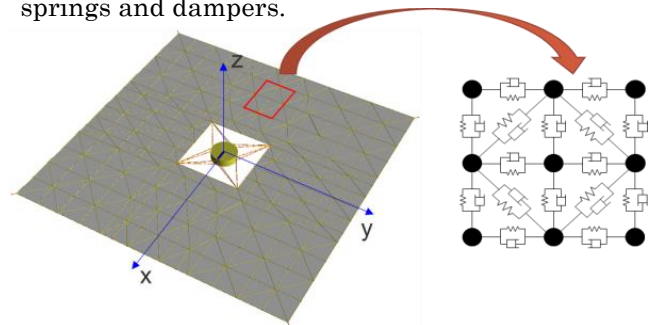


Fig.8 Concept of multi-particle method

The inter-particle force F can be obtained as follow;

$$F = \begin{cases} K(L - L_0) + \beta K\dot{L} & (L \geq L_0) \\ K\alpha(L - L_0) + \alpha\beta K\dot{L} & (L < L_0) \end{cases}$$

K , L , L_0 , α and β are defined as spring constant, natural length of spring, distance between two particles, coefficient of compression stiffness and coefficient of dumping, respectively.

By dividing the sail into triangular elements, these weights are distributed to each node. On the assumption that is equivalent to the strain energy which is derived from physical properties and elastic energy determined from the displacement of the mass, spring constant K is calculated. Coefficient of dumping is derived from the ratio of the spring constant. Assuming that the membrane resistance a compression slightly, nonlinear spring model using coefficients of compression stiffness are employed.

This model can take into account the effect of bending stiffness of each element. In addition, the SRP $4.57 \times 10^{-6}(N/m^2)$ of the anti-solar direction is also assumed as a force to give to each node.

4. Low Spin Operation

4-1. Image analysis result

From the analysis result as shown in Figure 9, the tip mass of the side of CAM-H1 and 3 are displaced upward. On the other hand, the tip mass of the side of CAM-H2 and 4 are displaced downward. In consequent, it can be estimated that the sail in the low spin operation change to saddle shape.

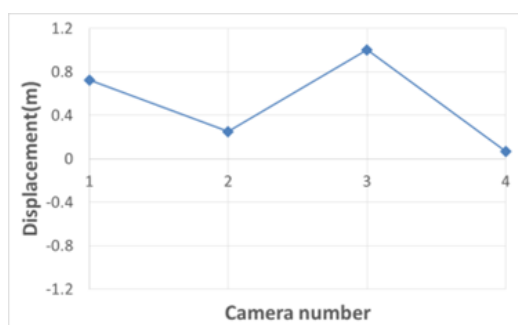


Fig.9 Displacement of tip mass in low spin operation

4-2. Set of stiffness

From the previous study, it has been shown that lower vibration mode of the sail is the saddle shape. Because of this, it is considered that the sail naturally deforms in the saddle shape under the only effect of the SRP and stiffness in the low-spin operation. Therefore, in order to simulate the model in detail, the stiffness is set four types in this analysis as shown in Figure 10, which are Fold line, Bridge, Edge processed tape, and Steering device. In addition, from the previous study, the stiffness value tends to be greater than the actual physical properties. Because of this, the value of the stiffness is set to a closed value to the simulation.

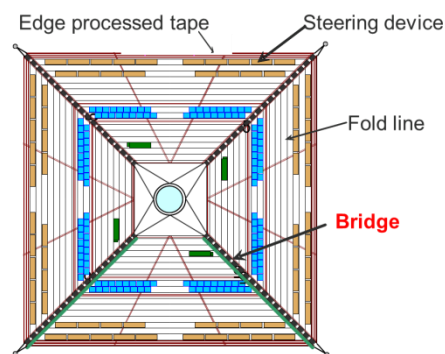


Fig.10 Stiffness of four types

4-3. Comparison with simulation result

Figure 11 is shown the comparison of the simulation result and the image analysis. It can be confirmed that the sail deforms of the same relative position, although there are some errors in the displacement of the tip mass. Furthermore, Figure 12 is shown the image of simulation result in the low spin operation.

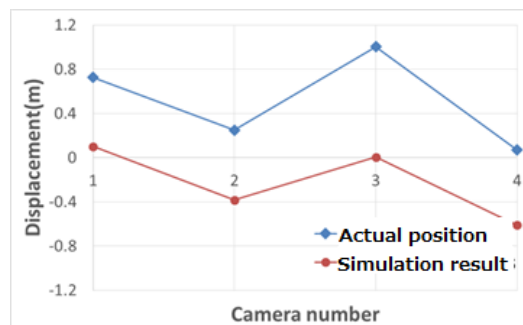


Fig.11 Displacement of tip mass in comparison of simulation and image analysis

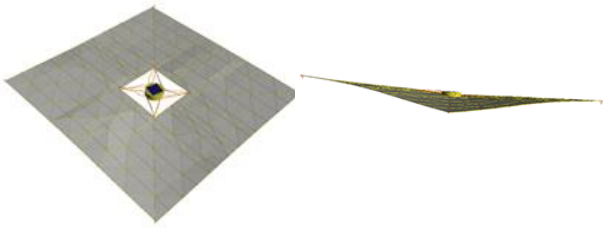


Fig.12 Image of simulation in low spin operation

From Figure 12, it can be considered that the sail deforms in a saddle shape from the relationship between the stiffness and the SRP in the low spin operation. In addition, it can be said to be able to make roughly estimation of the stiffness value by this analysis.

4-4. Additional study on stiffness

Because the sail shape of the simulation is almost contrast, there must have not been no factors that determine the deformed direction of the saddle shape. Therefore, it is evaluated that which factors largely determine the deformed direction of the saddle shape.

In this analysis, it is inferred that the stiffness of the bridge largely affects the deformed direction. Therefore, the value of the stiffness is changed to 0.9 times of the CAM-H1 and 3, and 1.1 times of the CAM-H2 and 4 than the previous stiffness as shown in Figure 13.

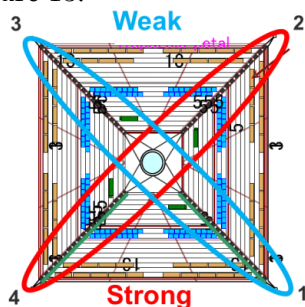


Fig.13 Adjustment of the bridge stiffness

Figure 14 is shown the result of the simulation. From Figure 14, the deformed direction of the saddle shape is the opposite of the previous direction. With this result, it can be confirmed that deformed direction of the saddle shape depends on a slightly difference in the bridge stiffness.

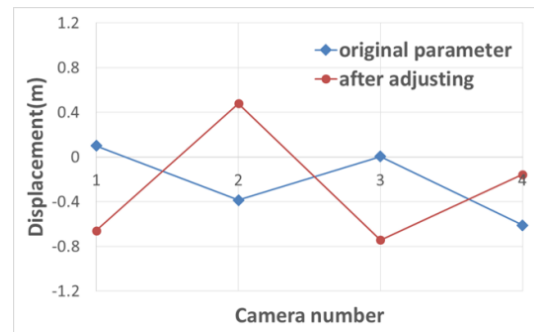


Fig.14 Displacement of tip mass in comparison with value of bridge stiffness

5. Reverse spin operation

5-1. Image analysis result

Figure 15 is shown the result of displacement of the tip mass from the pictures in the reverse and spin operation. Although both analysis are shown the deformation to the saddle shape, the direction is an opposite. From this result, it is inferred that there are other factors that make the deformation of the saddle shape cause in the reverse spin operation.

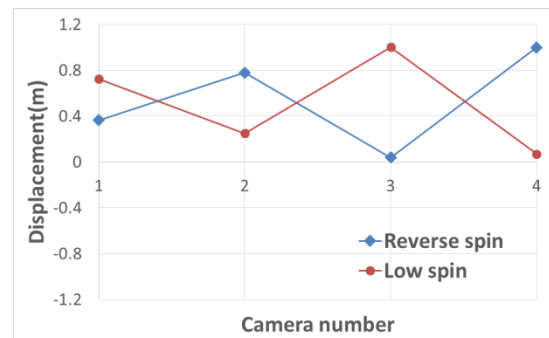


Fig.15 Displacement of tip mass in comparison of reverse and low spin operation

5-2. Effect of thruster plume

A major difference of the low and reverse spin operation is the effect of a thruster plume at the time to perform the spin rate control. The thruster plume blows in a vertical direction which lifts to the upper petal 2 and 4 as shown in Figure 16.

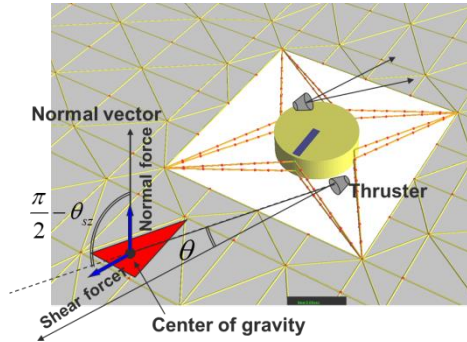


Fig.16 Affected part of thruster plume

In order to consider the effect of thruster plume, the plume is defined as a dilute fluid model.

The plume density can be obtained as follow;

$$\rho = \alpha \frac{\cos^{\beta} \left(\frac{\pi}{2} \frac{\theta}{\theta_{lim}} \right)}{r_{th}^2}$$

α and $\beta, \theta_{lim}, r_{th}$ are defined as constant, maximum expansion angle, distance to the plume, respectively.

The pressure of plume can be obtained as follow;

$$p = \frac{\rho U^2}{2S^2} \left[(2 - \delta) \{1 + 2(S \sin \theta_{sz})^2\} + \delta \sqrt{\frac{\pi T_w}{T}} S \sin \theta_{sz} \right]$$

δ, ρ, U, T, T_w are defined as coefficient of reflection, plume density, plume velocity, plume temperature, surface temperature, respectively.

5-3. Comparison with simulation result

Figure 17 is shown the comparison of the simulation result and the image analysis. It can be estimated that the sail deforms of the almost same relative position. Figure 18 is also shown the image of simulation in reverse spin operation.

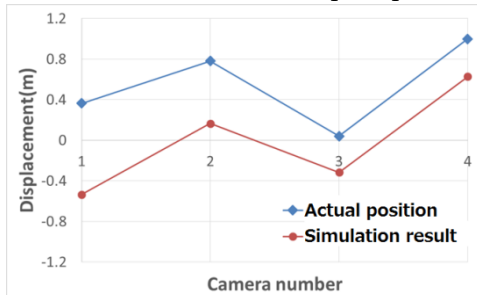


Fig.17 Displacement of tip mass in comparison of image analysis and simulation

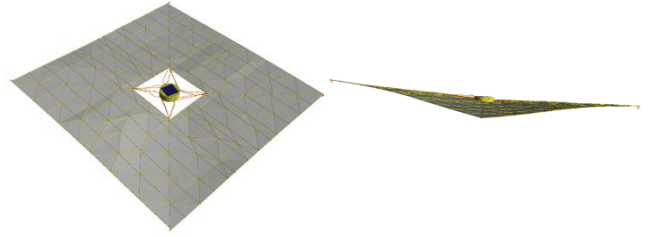


Fig.18 Image of simulation in reverse spin operation

From Figure 17, it can be confirmed that the effect of the plume thruster dominates the deformation behavior of the saddle shape in the reverse operation.

6. Conclusion

First, the deformation in the saddle shape can be confirmed quantitatively by image analysis.

Subsequently, in the low spin operation, it can be considered that the sail deforms in a saddle shape from the relationship between the stiffness and the SRP. On the other hand, in the reverse operation, it can be confirmed that the effect of the plume thruster dominates the deformation behavior of the saddle shape.

For these reasons, it can be concluded that IKAROS keeps the saddle shape without causing a large deformation in zero spin.

References

- 1)Kenji Kitamura, "Sail Shape Estimation of IKAROS Based on Flight Images", 日本航空宇宙学会論文集, Vol.57, No.660, 2012, pp.1-9.
- 2)Yoji Shirasawa, "Study on the effect of Bending Stiffness on the Membrane Dynamics of Solar Power Sail Demonstrator "IKAROS"", American institute of Aeronautics and Astronautics, 2008, pp.1-11.
- 3)Toshihiro Chujo, Y. Tsuda, and T. Saiki, "Solar Sail Attitude Dynamics Considering Sail Deformation", AAS Space Flight Mechanics Meeting, AAS13-759, Hilton head, 2013.